Fluctuation force exerted by a planar self-avoiding polymer

A Letters Journal Exploring the Frontiers of Physics

April 2009

EPL, **86** (2009) 22001
doi: 10.1209/0295-5075/86/22001

www.epljournal.org

Fluctuation force exerted by a planar self-avoiding polymer

P. Le Doussal and K. J. Wiese[a]

CNRS-Laboratoire de Physique Théorique de l'Ecole Normale Supérieure - 24 rue Lhomond, 75231 Paris Cedex, France, EU

received 9 December 2008; accepted in final form 16 March 2009
published online 30 April 2009

PACS 24.60.-k – Statistical theory and fluctuations
PACS 05.40.-a – Fluctuation phenomena, random processes, noise, and Brownian motion
PACS 66.30.hk – Polymers

Abstract – Using the results from Schramm Löwner evolution (SLE), we give the expression of the fluctuation-induced force exerted by a polymer on a small impenetrable disk, in various two-dimensional domain geometries. We generalize to two polymers and examine whether the fluctuation force can trap the object into a stable equilibrium. We compute the force exerted on the objects at the domain boundary, and the force mediated by the polymer between such objects. The results can straightforwardly be extended to any SLE interface, including Ising, percolation, and loop-erased random walks. Some are relevant for extremal value statistics.

What is the force exerted by a polymer on a small object such as a mesoscopic disk or a molecule? Simply because the object cannot be penetrated by the polymer it constrains its thermal fluctuations and feels an entropic force. This question is relevant in view of the recent surge of interest in fluctuation-induced forces, such as Casimir forces, triggered by beautiful experiments in critical systems [1]. Apart from Gaussian fluctuations, the calculation of Casimir forces is difficult, and it is useful to obtain exact results for non-trivial theories [2].

While there are many results available in two-dimensional critical systems, some obtained recently, originating from stochastic Löwner evolution (SLE) [3] (see [4,5] for review), their implications in terms of fluctuation-induced forces has, to our knowledge, not been discussed.

In this letter, we consider a polymer restricted, *e.g.*, by plates or through absorption [6], to a planar geometry, modeled by a self-avoiding walk (SAW) of N steps on a 2d lattice of spacing a. In the limit of large N and small a it is described by a continuum model. Start with a polymer with *one endpoint fixed*. Geometry $\mathcal{A}$ represented on the left side of fig. 1 is a half-plane where the polymer's end is fixed at the origin and free to wander to infinity. Then place a mesoscopic object, modeled by a disk of size ℓ, at point $z = x + \mathrm{i}y$. The object is impenetrable to the polymer, which is hence constrained to remain on the left of point z. We are interested in the free energy

$$\mathcal{F} = -kT \ln \mathcal{P}(z, \bar{z}). \tag{1}$$

[a] E-mail: wiese@lpt.ens.fr

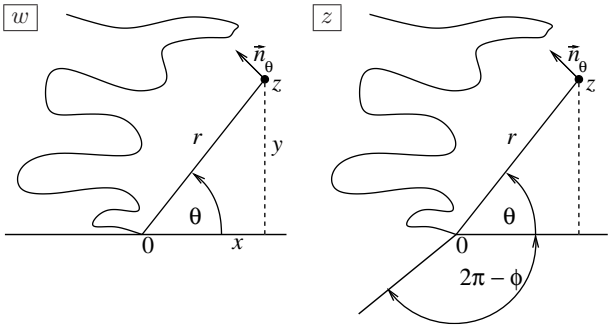

Fig. 1: (Left) Geometry $\mathcal{A}$: a self-avoiding polymer fixed at the origin and constrained to remain left of the point z. (Right) Geometry $\mathcal{B}$: same as $\mathcal{A}$, the polymer being fixed at the top of a wedge of exterior angle ϕ.

Here, $\mathcal{P}(z, \bar{z}) = Z(z, \bar{z})/Z$, where Z is the partition sum of the polymer in the absence of the object and $Z(z, \bar{z})$ is the constrained one. Since the SAW in the continuum limit is conjectured to be described by SLE with parameter $\kappa = 8/3$ [7,8], we can use $\mathcal{P}(z, \bar{z}) = \mathcal{P}_0(\theta)$ as given by Schramm's formula (for $\kappa = 8/3$) $\mathcal{P}_0(\theta) = \cos^2(\theta/2)$, where θ is the angle with the real axis (see fig. 1). From this we obtain the force exerted by the polymer on the impenetrable object:

$$\vec{f} = -\vec{\nabla} F = kT \frac{\vec{n}_\theta}{r} \frac{\partial}{\partial \theta} \ln \mathcal{P}_0(\theta) = -kT \frac{\vec{n}_\theta}{r} \tan\left(\frac{\theta}{2}\right). \tag{2}$$

This result is valid in the (critical) limit $a, \ell \ll r$, of object- and monomer-size small compared to r, and r small compared to the radius of gyration R_{g}, noting that

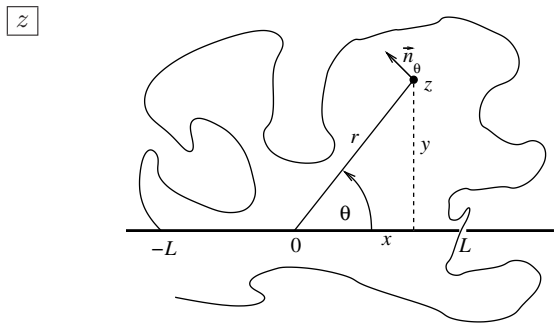

Fig. 2: Geometry $\mathcal{C}$: a self-avoiding polymer constrained to depart from $x=-L$, reaching $x=L$, and encircling both the origin and the point z.

SLE works at fixed chemical potential instead of fixed length [7,8]. When approaching the boundary on the $x<0$ side, the object is repelled by a force diverging as $2kT/y$, with y being the distance from the wall.

We can now use conformal invariance to obtain results in various geometries. The simplest one is the wedge geometry $\mathcal{B}$, see right side of fig. 1, with exterior angle ϕ, the polymer being attached at the top of the wedge. Under the map $w=g(z)=z^{\pi/\phi}$, the wedge geometry (in coordinate $z=x+\mathrm{i}y$) is mapped back to the half-plane (in coordinate w). The case $\phi=2\pi$ corresponds to the full plane with impenetrable positive real axis. Conformal invariance means that $\mathcal{P}(z,\bar{z})=\mathcal{P}_0(g(z),\overline{g(z)})$, where $\mathcal{P}_0$ is the upper-half-plane result given above. We find for the free energy and force

$$\mathcal{F}_{\mathcal{B}}=-kT\left[\ln(1+\cos(\alpha\theta))-\ln 2\right], \tag{3}$$

$$\vec{f}_{\mathcal{B}}=-kT\frac{\vec{n}_\theta}{r}\frac{\pi}{\phi}\tan(\pi\theta/2\phi). \tag{4}$$

Let us now study a polymer with *two endpoints fixed* as shown in fig. 2 (geometry $\mathcal{C}$). Since SLE describes the continuum limit of the SAW with fixed endpoints but fluctuating number of steps N at the critical chemical potential [7,8], a possible setting for an experiment is to consider the real axis as impenetrable, fix one endpoint at $x=-L$ and place a hole at $x=L$, through which the self-avoiding polymer passes. It is also possible to use two symmetric holes. Assuming equilibrium for an infinitely long polymer ensures that the chemical potential is at its critical value. In real experiments, N is always finite, though rather large DNA molecules exist, which could be used in an absorption experiment similar to [6], as long as $2L\ll R_{\mathrm{g}}$.

We can now use $w=g(z)=\frac{z+L}{L-z}$, which maps geometry $\mathcal{C}$ back to $\mathcal{A}$. It maps the half-plane onto itself, preserves the real axis, and maps $z=-L$ to $w=0$ and $z=L$ to infinity, hence back to fig. 1. Note that the segment $[-L,L]$ is mapped to the real positive w axis. Conformal invariance yields

$$\mathcal{F}_{\mathcal{C}}=-kT\left[\ln\left(\frac{\epsilon(L^2-r^2)}{\sqrt{r^4-2\cos(2\theta)r^2L^2+L^4}}+1\right)-\ln 2\right] \tag{5}$$

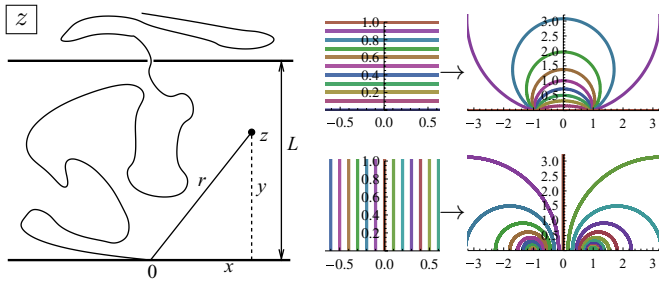

Fig. 3: (Color online) (Left) Strip geometry $\mathcal{D}$: a self-avoiding polymer constrained to depart from $x=0$, passing through $x=\mathrm{i}L$, and staying left of point z. (Right): mapping of the strip to the plane.

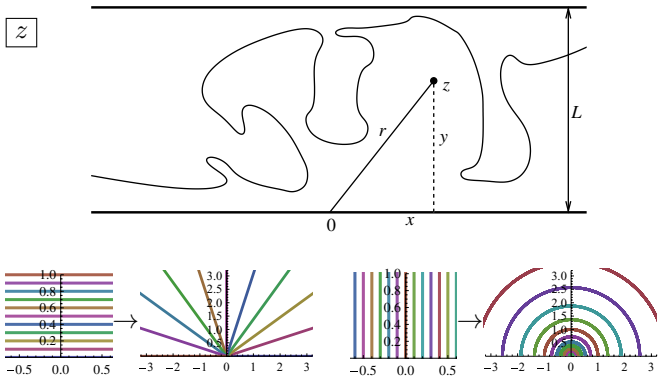

Fig. 4: (Color online) (Top) Strip geometry $\mathcal{E}$: a self-avoiding polymer constrained to depart from $x=-\infty$, going to $x=+\infty$, and passing at the top of point z. (Bottom): mapping of the strip to the plane.

with $\epsilon=1$ if the object is inside the area encircled by the polymer and $\epsilon=-1$ if it is outside. Computing the force, one finds that for $\theta=\pi/2$ the force is radial $f_r=-2\epsilon kT/[r(1+r^2/L^2)]$ and crosses over from $1/r$ to L^2/r^3 as r increases, being attractive if the object is inside, repulsive if it is outside.

Instead of a half-plane, one can compute the force in any singly connected domain as, *e.g.*, a disk or a strip. We consider two distinct infinite strip geometries $z=x+\mathrm{i}y$. In the first strip geometry, $\mathcal{D}$, presented in fig. 3, the strip is $0\leqslant y\leqslant L$ and the polymer is attached at $z=0$ and $z=\mathrm{i}L$ (in the sense defined above, *i.e.*, passing through a hole at $Z=\mathrm{i}L$). Using $w=\tanh(\pi z/(2L))=(\mathrm{e}^{\pi z/L}-1)/(\mathrm{e}^{\pi z/L}+1)$ to map it to geometry $\mathcal{A}$ of fig. 1, one finds the free energy in geometry $\mathcal{D}$

$$\mathcal{F}_{\mathcal{D}}=-kT\ln\left[\frac{1}{2}+\frac{1}{2}\frac{\sqrt{2}\sinh(\pi x/L)}{\sqrt{\cosh(2\pi x/L)-\cos(2\pi y/L)}}\right]. \tag{6}$$

On the symmetric line $y=L/2$, the force is directed along x and equal to $f_x=\frac{kT}{L}\frac{2\pi}{1+\mathrm{e}^{2\pi x/L}}$, which has a finite limit at large negative x.

In the second strip geometry, $\mathcal{E}$ in fig. 4, the polymer is attached infinitely far away on each side and the object is below it. Using the map $w=\mathrm{e}^{\pi z/L}$, one finds the free

energy and force (with $f_x = 0$)

$$\mathcal{F}_{\mathcal{E}} = -kT\Big[\ln\left(1+\cos(\pi y/L)\right) - \ln 2\Big], \tag{7}$$

$$f_y^{\mathcal{E}} = -\frac{\pi}{L}\tan\Big(\frac{\pi y}{2L}\Big). \tag{8}$$

In all cases considered above, the force tends to bring the object toward a portion of the boundary. One can ask whether it is possible to levitate the object into a stable equilibrium away from the boundaries. For this, one needs (at least) two polymers. This more difficult problem was solved when the two polymers start at the same point or nearby on the real axis and both go to infinity [9]. We use their extension of Schramm's formula to two SLEs conditioned not to merge before reaching infinity. One defines $\mathcal{P}_{\rm l}$, $\mathcal{P}_{\rm m}$ and $\mathcal{P}_{\rm r} = 1 - \mathcal{P}_{\rm m} - \mathcal{P}_{\rm l}$ the relative weights of configurations such that the object is constrained to lie on the left of both the polymers (l), in the middle (m) or to the right (r). Then, $\mathcal{P}_{\rm m} = \frac{4}{5}\sin^2(\theta)$. Hence, the free energy is

$$\mathcal{F}_{\rm m} = -kT\left[2\ln(\sin\theta) + \ln(4/5)\right]. \tag{9}$$

More complicated formulas hold for $\mathcal{P}_{\rm r}$ and $\mathcal{F}_{\rm r}$. We obtain for the force exerted on a point, which remains to the left of the two polymers (l), in the middle (m) or to the right (r) as $\vec{f} = f^\theta \vec{n}_\theta$ with

$$\begin{aligned} f^\theta_{\rm l} &= -\frac{kT}{r}\frac{8\sin(\theta)\Big[-12\theta\cos(\theta)+9\sin(\theta)+\sin(3\theta)\Big]}{-24\cos(2\theta)\theta - 36\theta + 28\sin(2\theta)+\sin(4\theta)}, \\ f^\theta_{\rm m} &= \frac{kT}{r}2\cot(\theta), \end{aligned} \tag{10}$$

and $f^\theta_{\rm r}(\theta) = -f^\theta_{\rm l}(\pi-\theta)$. This is plotted in fig. 5. Note that, when the object is trapped in the middle of the two polymers, the symmetry line $\theta = \pi/2$ is a line of equilibrium points, stable in the angular direction and neutral in the radial one. Hence, the object is brought back to the symmetry line and force flow lines are circles $r = cst$ heading toward $\theta = \pi/2$. A remarkable property holds

$$\mathcal{P}_{\rm m}(z,\bar{z}) = \frac{16}{5}\mathcal{P}^{(1)}_{\rm l}(z,\bar{z})\mathcal{P}^{(1)}_{\rm r}(z,\bar{z}), \tag{11}$$

where $\mathcal{P}^{(1)}_{\rm l/r}$ is the (Schramm) probability for a single self-avoiding polymer to pass left/right of the point. Hence, if the point is in the middle, the fluctuation force is *the same* as for two independent polymers, *i.e.*, mutual avoidance does not change the result, as can be checked on (10). This is *not true* if the polymers are on the same side of the object.

Let us consider again the geometry of fig. 2 now with both the polymers attached at $x = -L$, and both passing through a hole at $x = L$, see top right of fig. 5. An object trapped in the middle acquires a free energy

$$\mathcal{F}_{\rm m} = -kT\log\left(\frac{16r^2L^2\sin^2(\theta)}{5\left(r^4 - 2\cos(2\theta)r^2L^2 + L^4\right)}\right). \tag{12}$$

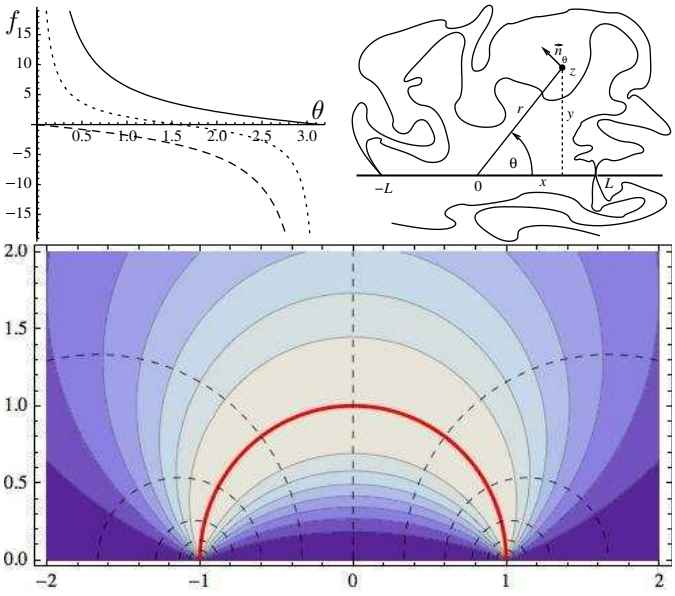

Fig. 5: (Color online) (Top left): force along $\vec{n}_\theta$ exerted by two self-avoiding polymers on a point object, if the object is left of the two polymers (solid), between them (dashed) or right of them (dotted), in geometry $\mathcal{A}$. (Top right) Geometry $\mathcal{C}$: two self-avoiding polymers fixed at $-L$, passing through a hole at L, and constrained to remain above and below the point z. (Bottom): equal probability lines (solid) and force flow lines (dashed) for geometry $\mathcal{F}$; plot-units are L.

The equipotential lines are given at the bottom of fig. 5, with the minimum on the circle of radius L, passing through $\pm L$ (bold red). This leads to a force

$$\vec{f}_{\rm m} = \frac{2kT}{r}\frac{(L^4 - r^4)\vec{n}_r + (r^2 - L^2)^2\cot(\theta)\vec{n}_\theta}{L^4 + r^4 - 2r^2L^2\cos(2\theta)}, \tag{13}$$

which due to (11) is the sum of the forces of two independent SAWs. There is now a semi-circle of equilibrium points $r = L$, which is the image of the vertical straight line passing through 0 of geometry $\mathcal{A}$. Note that there is no force on the line, thus no *stable* equilibrium.

We now argue that trapping occurs in two cases: i) a finite-size object, *e.g.*, a small disk and ii) a point submitted to a thermal bath. From scale invariance, the probability $\mathcal{P}_{\rm m}(\phi)$ that two SAWs starting at 0 avoid a disk with center on the imaginary axis, and pass one to the left and one to the right, depends only on the angle ϕ of the cone shown on the left side of fig. 6 and is clearly a decreasing function of ϕ, with $\mathcal{P}_{\rm m}(0) = \mathcal{P}_{\rm m}$ and $\mathcal{P}_{\rm m}(\pi) = 0$. Hence, a disk of fixed size will be pushed to infinity along the imaginary axis. Under conformal mapping of geometry $\mathcal{A}$ to $\mathcal{C}$, disks map to disks and the cone to the space between two circular arcs. Assuming conformal invariance of the probabilities, all disks shown in fig. 6 have the same free energy. The center of a disk will thus be pushed to the stable equilibrium point above the origin, where the largest disk is drawn. A quantitative result is possible for small radius ρ. For example, in the geometry

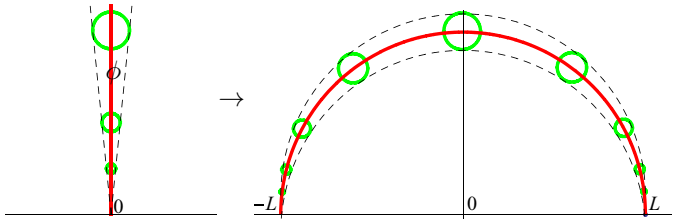

Fig. 6: (Color online) Mapping of self-avoiding walks constrained to pass to the left and to the right of disks from geometry $\mathcal{A}$ to geometry $\mathcal{C}$: all disks drawn correspond to the same probability, *i.e.*, same free energy.

$\mathcal{A}$ the no-hit probability for a disk centered at $x+\mathrm{i}y$ reads $p \approx 1 - c(\frac{\rho}{2y})^{2/3}\sin^2(\theta)$ to lowest order in powers of ρ/y, as extracted from [4,10,11], with an unknown constant c. This gives the force $kT\vec{\nabla}\ln p$. In the symmetric case $\theta=\pi/2$, the force along the radial direction is

$$f_r \approx \frac{2ckT}{3}\frac{1}{r}\left(\frac{\rho}{2r}\right)^{2/3}, \tag{14}$$

which decays as $1/r^{5/3}$ at large distances.

Now, consider a point-like object subjected to the Casimir force above plus a thermal bath at temperature T'. The equilibrium Gibbs measure for the object is $\mathcal{P}=\mathcal{P}(z,\bar{z})^{T/T'}/\mathcal{Z}$, and the partition sum of polymer plus object is $\mathcal{Z}=\int \mathrm{d}^2z\,\mathcal{P}(z,\bar{z})^{T/T'}$. Here, $\mathcal{P}$ is either Schramm's probability $\mathcal{P}_0$ for a single polymer, as given in the text above eq. (2), or $\mathcal{P}_{\rm m}$ in eq. (11) for an object caught between two SAWs. For the latter case, equiprobability lines are plotted at the bottom of fig. 5 for $T'=T$. Depending on the geometry and T/T', $\mathcal{Z}$ is either infinite, and the object diffuses to the region where the integral is divergent, or finite and the object is bound. The latter occurs for any $T'<T$ in geometry $\mathcal{C}$ (top right of fig. 5), since at large r, $\mathcal{P}\mathrm{d}^2z \sim \mathrm{d}\theta\, r\mathrm{d}r(\sin^2(\theta)/r^2)^{T/T'}$. For $T=T'$, a natural choice when the two polymers and the object are in mutual thermal equilibrium, this geometry is critical, hence the object diffuses to infinity. Other geometries, however, exhibit a bound state for $T=T'$. For example, the strip geometry $\mathcal{D}$ has a normalizable distribution

$$\mathcal{P}_{\rm m} = \frac{\pi}{L^2\ln 2}\frac{\sin^2(\pi y/L)}{\cosh(2\pi x/L)-\cos(2\pi y/L)}, \tag{15}$$

and an exponentially localized bound state, with the length set by the strip width. An algebraic bound state is obtained if, in fig. 5 with the two polymers going through $-L$ and L, one rotates the real negative axis around 0 clockwise to form a wedge with angle $\phi<\pi$. Then

$$\mathcal{P}_{\rm m}(r,\theta) = \mathcal{N}_a\frac{L^{2a-2}r^{2a}\sin^2(a\theta)}{L^{4a}+r^{4a}-2(rL)^{2a}\cos(2a\theta)} \tag{16}$$

with $a=\pi/\phi>1$ (the formula remains true for $a<1$ as a non-normalizable density) and $\pi\mathcal{N}_a = 4a^2/(\psi(\frac{1}{2a})-\psi(\frac{1}{2}+\frac{1}{2a})+a+(\pi/\sin(\frac{\pi}{a}))$.

Let us compare the force exerted by one and by two polymers. Let us choose the simplest geometry $\mathcal{E}$, the infinite strip with the two polymers attached at both ends (fig. 4), where the force is along y. For an object in the middle, one has a restoring force toward the neutral axis $y=L/2$

$$f_y^{\rm m} = \frac{2kT\pi}{L}\cot\Big(\frac{\pi y}{L}\Big), \tag{17}$$

while the force exerted by two polymers is $f_y = kT\partial_y\ln\mathcal{P}$,

$$\mathcal{P} = 24\pi\cos\left(\tfrac{2\pi y}{L}\right)\left(1-\tfrac{y}{L}\right)+36\pi\left(1-\tfrac{y}{L}\right)+28\sin\left(\tfrac{2\pi y}{L}\right) + \sin\left(\tfrac{4\pi y}{L}\right). \tag{18}$$

Its ratio to the force, (8), exerted by a single polymer increases monotonically from $\frac{16}{5}$ (at $y=0$) to $\frac{7}{2}$ (at $y=L$). For an interpretation of the first number see below.

We can now compute the force exerted by a single polymer on an object placed on the boundary of the system (*e.g.*, the upper half-plane H). We use the nice result of [8] arising from the so-called restriction property obeyed by SAWs. It states that the probability that a SAW (from 0 to infinity) does not visit a subdomain A is $|g_A'(0)|^{5/8}$, where g_A is the map from $H\backslash A$ to H, which removes A and has $g_A(0)=0$, and $g_A(z)\sim z$ at infinity. Note that $H\backslash A$ must be singly connected, hence the object connected to the boundary. For a general domain D and endpoints a and b on the boundary the probability is $|g_A'(a)|^{5/8}|g_A'(b)|^{5/8}$ with $g_A(a)=a$ and $g_B(b)=b$. Note that a similar result holds for a Brownian excursion, *i.e.*, a Brownian from a to b conditioned not to hit the boundary, with the exponent $5/8$ replaced by 1. Finally, let us mention that for a SAW from point a on the boundary to point b in the bulk (radial SLE), the probability becomes $|g_A'(a)|^{5/8}|g_A'(b)|^{5/48}$. In CFT language, $h_{1,2}$ (with $h_{1,2}=5/8$ for $\kappa=8/3$) is the dimension of the operator Φ_{12} creating a curve on the boundary, $2h_{0,1/2}=5/48$ is the dimension of the bulk operator $\Phi_{0,1/2}$ creating a curve in the bulk. $\Phi_{1,3}$ with $h_{1,3}=2$ creates two curves on the boundary conditioned not to annihilate. When generalized, this implies that the force exerted by n polymers with identical endpoints on a given subdomain A connected to the boundary is proportional to $h_{1,n+1}=n(3n+2)/8$, which explains the ratio $h_{1,3}/h_{1,2}=16/5$ found above, see eq. (18), for small y (point close to the boundary)[1].

The simplest example for an object A connected to the boundary is a vertical segment $z=a+\mathrm{i}y$ with $y\in[0,h]$, which is removed by the map $g_A(z)=\sqrt{(z-a)^2+h^2}+\mathrm{sign}(a)\sqrt{a^2+h^2}$. The no-hit probability is $\mathcal{P}=\left(\frac{a^2}{h^2+a^2}\right)^{5/16}$, and the total force $\vec{f}=kT\vec{\nabla}\ln\mathcal{P}$ is

$$f_x = \frac{5}{8}kT\frac{h^2}{a(a^2+h^2)}, \qquad f_y = -\frac{5}{8}kT\frac{h}{(a^2+h^2)}. \tag{19}$$

To obtain the force when the polymer starts at 0 and ends at $z_0=x_0+\mathrm{i}y_0$ in the half-plane, one uses the map

[1] For n polymers ending in the bulk the exponent $5/48$ is replaced by $2h_{0,n/2}=\frac{3}{8}(\frac{n^2}{4}-\frac{1}{9})$.

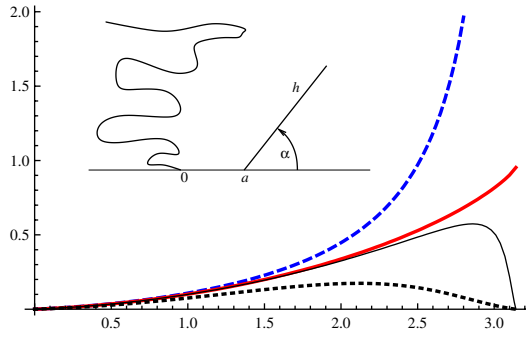

Fig. 7: (Color online) Inset: closing-door geometry. Main plot: h/a times the free energy, *i.e.*, $\frac{h}{a}\mathcal{F}$ (in units of kT) for this geometry, as a function of α. The curves are (from top to bottom): $h/a=2$ (dashed blue), $h/a=1$ (thick, solid, red), $h/a=0.95$ (thin, solid, black), $h/a=1/2$ (dotted, thick, black). The last point on $h/a=1$ curve is obtained analytically in (23).

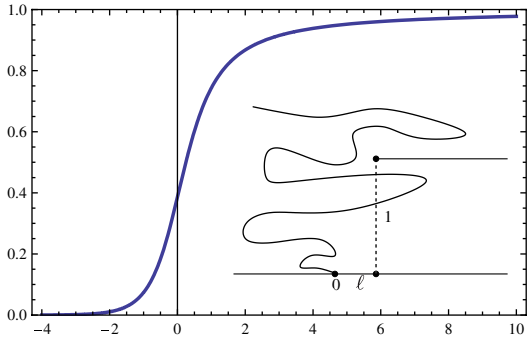

Fig. 8: (Color online) The probability to avoid a wall starting from $(\ell,1)$ to $(\infty,1)$. Inset: the geometry in question.

$v=\tilde{g}_A(z)$, which preserves z_0 rather than ∞. Composing g_A with a Moebius map that maps H to H, 0 to 0, and $g(z_0)$ back to z_0, one finds a complicated formula that simplifies for $x_0=a$ to $\mathcal{P}=(\frac{a^2}{a^2+h^2})^{\frac{5}{16}}y_0^{-5/12}(y_0^2-h^2)^{5/24}$. This gives for the force on the wall $f_y=-\frac{5kT}{24}(\frac{3h}{a^2+h^2}+\frac{2h}{y_0^2-h^2})$, which diverges as $y_0\to h^+$.

Another example is a half-disk of radius r centered at $x=a>0$. The uniformizing map is $g(z)=z+\frac{r^2}{a}+\frac{r^2}{z-a}$. Hence, the no-hit probability is $\mathcal{P}=(1-\frac{r^2}{a^2})^{5/8}$, and the object is repelled with a force $f_x=\frac{5kT}{4a}r^2/(a^2-r^2)$.

The *polymer piston* is interesting for *extreme-value statistics*. Consider the strip geometry $\mathcal{D}$ in fig. 3 and add an impenetrable region P (the piston) for $x>a$. The map $h_a(z)=[\cosh(\frac{\pi}{L}a)-\cosh(\frac{\pi}{L}(z-a))]/[\cosh(\frac{\pi}{L}(z-a))+\cosh(\frac{\pi}{L}a)]$ maps the strip minus P to the upper half-plane, and both axes $y=0$ and $y=L$ to 0. Hence, the map that removes the piston is $g_A(z)=h_\infty^{-1}(h_a(z))=(L/\pi)\ln(\cosh(\pi(z-a)/L)/\cosh(a\pi/L))$ while leaving 0 and iL fixed. The no-hit probability is

$$\mathcal{P}=|g_A'(0)|^{5/8}|g_A'(\mathrm{i}L)|^{5/8}=[\tanh(a\pi/L)]^{5/4}. \qquad (20)$$

Note that this is also the cumulative distribution of $x_{\max}=a$, the *maximum excursion of a SAW*. The total force exerted on the piston is $f_x=5\pi/[2L\sinh(2a\pi/L)]$.

Consider now the "door" geometry, *i.e.*, a segment $z=a+t\mathrm{e}^{\mathrm{i}\alpha}$ with $t\in[0,h]$, of angle $\alpha=b\pi$. The relevant map $w=g(z)$ has an explicit form in terms of its inverse map $z=f(w)$ with $f(w)=a+(w-x_1)[(w-x_3)/(w-x_1)]^b$, $0<x_1<x_3$ with $a=x_1(x_3/x_1)^b$ and $h=b^b(1-b)^{1-b}(x_3-x_1)$. The no-hit probability is

$$\mathcal{P}=\left[\mu^b(1-b(1-\mu^{-1}))\right]^{-5/8}, \qquad (21)$$

$$h/a=b^b(1-b)^{1-b}\mu^{-b}(\mu-1), \qquad (22)$$

where $\mu=x_3/x_1>1$ is the solution of eq. (22). The numerical solution is given in fig. 7. An interesting limit is represented in fig. 8, where $h=1/\sin(\pi k)$, $a=\ell+\cot(\pi k)$ and $k=1-b$ tends to zero. One finds that $\mu=\frac{1}{wk}+\mathrm{O}(k^0)$ with $w=W(\mathrm{e}^{\ell\pi-1})$ the product-log function $W(z)$ solution of $z=W\mathrm{e}^W$. This gives the no-hit probability of the horizontal half-line $\mathrm{i}+x$ with $x>\ell$, plotted in fig. 8,

$$\mathcal{P}=\left[1+\frac{1}{W\left(\mathrm{e}^{\ell\pi-1}\right)}\right]^{-5/8}. \qquad (23)$$

Let us now consider the fluctuation force between two objects, here two identical slits, *mediated by the polymer*, here in the symmetric position (see fig. 9). Following [12], the map which produces two slits is for $x_1<x_2<x_3$: $f'(w)=\frac{w^2-x_2^2}{\sqrt{w^2-x_1^2}\sqrt{w^2-x_3^2}}$, $f(w)=E\left(\arcsin(\frac{w}{x_1})|\frac{x_1^2}{x_3^2}\right)x_3+F\left(\arcsin(\frac{w}{x_1})|\frac{x_1^2}{x_3^2}\right)(x_2^2-x_3^2)/x_3$, where E, F, and K (below) are the elliptic E, F, and K functions, and our choice is $g(0)=0=f(0)$. The condition that $f(x_1)=f(x_3)$, or equivalently that $\Im f(x_3)=0$ yields a non-trivial condition. Define $\alpha=x_1/x_3$, $\beta=x_2/x_3$. Then, for $0<\alpha<\beta<1$: $\beta(\alpha)=\sqrt{\frac{E(\alpha^2)-E\left(\arcsin(\frac{1}{\alpha})|\alpha^2\right)}{F\left(\arcsin(\frac{1}{\alpha})|\alpha^2\right)-K(\alpha^2)}+1}$. The walls have position $\pm a$ and height h (see fig. 9)

$$a=f(x_1)=\left[E\left(\alpha^2\right)+\left(\beta^2-1\right)K\left(\alpha^2\right)\right]x_3, \qquad (24)$$

$$h=\Im f(x_2)=\Im\Big[E\left(\arcsin(\tfrac{\beta}{\alpha})|\alpha^2\right)+\left(\beta^2-1\right)F\left(\arcsin(\tfrac{\beta}{\alpha})|\alpha^2\right)\Big]x_3. \qquad (25)$$

The probability is $\mathcal{P}=|f'(0)|^{-\frac{5}{8}}=|\frac{\alpha}{\beta^2}|^{\frac{5}{8}}$. Figure 10 shows a parametric plot of $\mathcal{P}$, and of the interaction energy, as a function of h/a.

Consider now a small smooth object described by $z=x+\mathrm{i}y$, $0<y\leqslant Y(x)$, away from the origin, *i.e.*, $Y(0)=Y(\infty)=0$. If we find a function $f(t)$ with only positive Fourier components f_k, such that $x=x(t)=\Re f(t)$, $Y(x)=\Im f(t)$ describes the boundary for t real, then $f(z)=z+\int_{k>0}f_k\mathrm{e}^{\mathrm{i}kz}=z+\frac{1}{\pi}\int_t\frac{Y(x(t))}{t-z}$ is the inverse uniformizing map. In an expansion in powers of $Y(x)$ *and its derivatives* one finds $f(z)=\tilde{f}(z)-\tilde{f}(0)$ with $\tilde{f}(z)=z+\frac{1}{\pi}\int_t\frac{Y(t)}{t-z}-\frac{1}{2\pi^2}\int_{t,t'}Y'(t)Y'(t')(\frac{1}{t-z}+\frac{1}{t'-z})\ln|t-t'|+\ldots$.

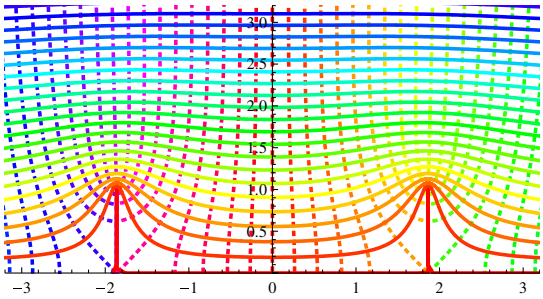

Fig. 9: (Color online) Image of the upper half-plane, and of lines parallel to the real axis (in thick), respectively imaginary (dotted), under the map $f(w)$ discussed in the text, which creates two slits, with $x_1 = 1$, $x_2 = 1.991$, and x_3=3.

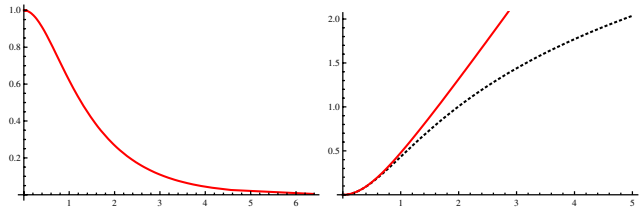

Fig. 10: (Color online) (Left): the probability that a polymer does not touch two slits, as a function of h/a for the geometry of fig. 9. (Right): the free energy in units of kT (solid line), compared to the sum of the free energies for a slit left and a slit right (dashed line), as a function of h/a. The difference is the interaction free energy mediated by the polymer.

This yields the free energy

$$\mathcal{F} = kT\frac{5}{8\pi}\left[\int_t \frac{Y(t)}{t^2} - \int_{t,t'} \mathcal{G}(t,t')Y'(t)Y'(t') + \dots\right], \tag{26}$$

where $2\pi\mathcal{G}(t,t') = (t^{-2}+t'^{-2})\ln|t-t'| + 1/(tt')$. For a single object centered at position a, $Y(t) = h(t-a)$, the repulsive force $f_x = -\partial_a\mathcal{F}$ decays as $f_x \approx 5kTA/(4\pi a^3)$ at large distances, with a prefactor $A = \int_t Y(x(t)) = \int_t h(t) - \frac{1}{\pi}\int_{tt'} h'(t)h'(t')\ln|t-t'| + \mathrm{O}(h^3)$. In the case of two objects, (26) yields their interaction, to lowest order, mediated by the polymer. For small objects, one finds $\mathcal{F}_{\rm int} = -kT\frac{5}{4\pi}\partial_a\partial_b\mathcal{G}(a,b)\int_t h_a(t)\int_{t'} h_b(t')$.

The interaction of a small object at z in the bulk with an arbitrary object on the boundary removed by the map $g(z)$ is obtained from the left passage probability $\mathcal{P}$, generalizing Schramm's formula to $\mathcal{P} = |g'(0)|^{\frac{5}{8}}\frac{1}{2}\left[1 + \frac{\Re g(z)}{|g(z)|}\right]$.

The previous calculations can be extended to fluctuation forces for an object impenetrable to the interface described by SLE for any κ. For illustration, the force in geometry $\mathcal{A}$ at $\theta = \pi/2$ reads

$$\vec{f} = -kT\frac{\vec{n}_\theta}{r}\frac{2\,\Gamma\left(\frac{4}{\kappa}\right)}{\sqrt{\pi}\,\Gamma\left(\frac{4}{\kappa}-\frac{1}{2}\right)}. \tag{27}$$

Extension to Ising at T_c assumes that the object interacts only with the interface induced by changes in boundary conditions, not the bubbles proliferating at criticality, which seems artificial. Physically meaningful is the polymer at the Θ point [13], conjectured to correspond to $\kappa = 6$. Further results follow from recent works: i) From [14] one obtains the force exerted by a loop-erased random walk ($\kappa = 2$) on an object of arbitrary shape. ii) From the *double* left-passage probability of a SAW [15] around points z_1, z_2 one computes the Casimir interaction between two points. Interestingly, when they are close and away from the boundary the interaction force is *attractive* and diverges for $y \approx y_1 \approx y_2$, $\theta \approx \theta_1 \approx \theta_2$ as $|f| \sim kTA(1-\cos\theta)y^{-2/3}|z_1 - z_2|^{-1/3}$ with $A = -\sqrt{3\pi}\Gamma(5/6)/[3\Gamma(-2/3)] = 0.287457\dots$. Near the boundary for small $y_1 = y_2 = y$, $\mathcal{F}_{\rm int} = -kTy^4/(5x_1x_2(x_1-x_2)^2) + \mathrm{O}(y^6)$, a *repulsive* interaction for $x_1 < x_2/3$.

* * *

We thank M. Bauer, D. Bernard, T. Emig, C. Hagendorf, Y. Kantor, and M. Kardar for useful discussions. This work was supported by ANR under program 05-BLAN-0099-01, and in part through NSF Grant PHY05-51164 during the program Fluctuate08 at KITP.

REFERENCES

[1] Garcia R. and Chan M. H. W., *Phys. Rev. Lett.*, **83** (1999) 1187; **88** (2002) 086101; Ganshin A. *et al.*, *Phys. Rev. Lett.*, **97** (2006) 075301; Mukhopadhyay A. and Law B. M., *Phys. Rev. Lett.*, **83** (1999) 772; Ueno T. *et al.*, *Phys. Rev. Lett.*, **90** (2003) 116102; Ishiguro R. and Balibar S., *J. Low Temp. Phys.*, **140** (2005) 29.
[2] Fisher M. E. and de Gennes P. G., *C. R. Acad. Sci. Paris Ser. B*, **287** (1978) 207; Krech M., *The Casimir Effect in Critical Systems* (World Scientific, Singapore) 1994; *J. Phys. Condens. Matter*, **11** (1999) R391; Nightingale M. P. and Indekeu J. O., *Phys. Rev. Lett.*, **54** (1985) 1824; Krech M. and Dietrich S., *Phys. Rev. Lett.*, **66** (1991) 345; **67** (1991) 1055.
[3] Schramm O., *Isr. J. Math.*, **118** (2000) 221.
[4] Cardy J., *Ann. Phys. (N.Y.)*, **318** (2005) 81.
[5] Bauer M. and Bernard D., *Phys. Rep.*, **432** (2006) 115.
[6] Ercolini E. *et al.*, *Phys. Rev. Lett.*, **98** (2007) 058102.
[7] Kennedy T., *J. Stat. Phys.*, **114** (2004) 51.
[8] Lawler G. F., Schramm O. and Werner W., *Proceedings of the Symposium on Pure Mathematics*, Vol. **72**. Part 2 (AMS, Providence, RI) 2004, pp. 339–364, arXiv:math/0204277; *J. Am. Math. Soc.*, **16** (2003) 917.
[9] Gamsa A. and Cardy J., *J. Stat. Mech.* (2005) P12009.
[10] Beffara V., *Ann. Probab.*, **36** (2008) 1421, arXiv:math/0211322.
[11] Bauer R. O., *Stoch. Processes Appl.*, **117** (2007) 1165, arXiv:math/0602391.
[12] Ahlfors L. V., *Complex Analysis* (McGraw-Hill, New York) 1979.
[13] Duplantier B. and Saleur H., *Phys. Rev. Lett.*, **59** (1987) 539; **61** (1988) 1521; Seno F. *et al.*, *Phys. Rev. Lett.*, **61** (1988) 1520.
[14] Hagendorf C., arXiv:0810.4503.
[15] Simmons J. H. and Cardy J., arXiv:0811.4767.